Kevin Anthony Pinks: MS 2020

Thesis "SYNTHESIS, CHARACTERIZATION AND BIOLOGICAL STUDIES OF NOVEL ORGANOANTIMONY(V) CYANOXIMATES."

I invited Kevin to work in my research lab in 2017 after I observed him in classes I taught that year. As undergraduate student he agreed to come and work on a brand new research project that I just started to develop. That is development of chemistry of novel organoantimony(V) compounds based on biologically active cyanoximes. Later that year I applied for the Faculty Research Grant (from the MSU Graduate College) and received funding for it including a stipend for a student. The first pioneering work with antimony I did two decades ago and it culminated in one major publication with my last Ph.D. student from Ukraine – Dr. Konstantin Domasevitch:

K.V. Domasevitch, N.N. Gerasimchuk, A.A. Mokhir. "Organoantimony(V) cyanoximates: synthesis, spectra and crystal structures." *Inorganic Chemistry*. **2000**, *39*, N^{o}6, p.1227- 1237.

This work with time received significant citations and now is ranked #6 with 75 citations in my list of the most cited publications. I wanted to continue exploration in this area and needed a student.

The project was designed to synthesize a series of tetraphenylantimony(V) cyanoximates, characterize them using X-ray crystallography and spectroscopy, make assessment of their thermal stability in solid state and solutions and then forward to collaborative institution for evaluation of their antimicrobial activity.

A series of ligands to be covalently bonded to the tetraphenylantimony(V) moiety is shown below in Figure 1:

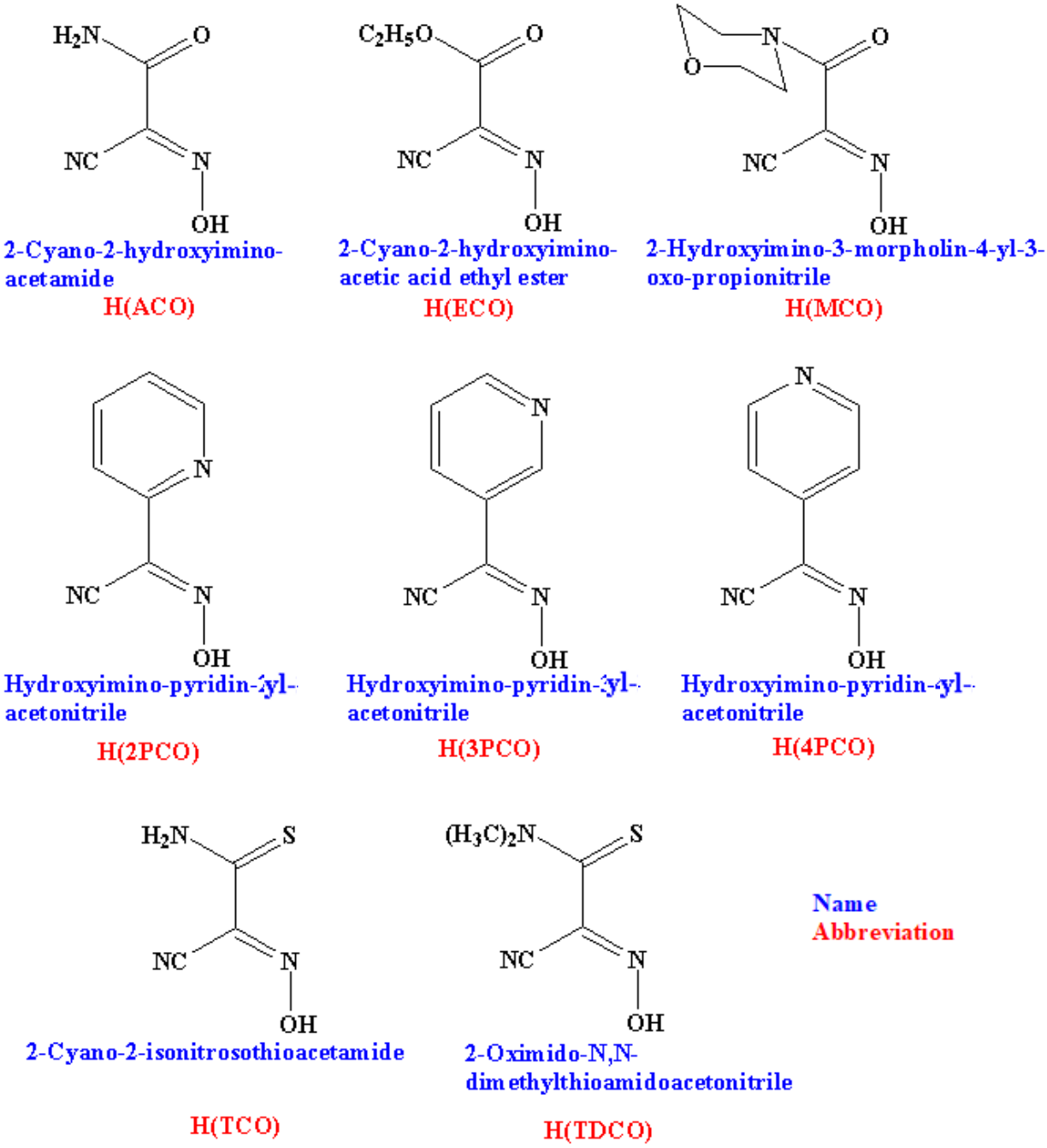

Figure 1. Chemical structures of selected cyanoxime ligands and their commonly used in our research laboratory abbreviations.

ABSTRACT

The requirement of new antimicrobial treatments has become an urgent field in the last two decades. Multi-drug resistant (MDR) bacteria are now resistant to common antibiotics such as penicillin, cephalosporin, and carbapenems. To antagonize such bacteria 8 novel organoantimony(V) cyanoximates were synthesized with the purpose to be characterized and submitted for biological activity studies. The eight organoantimony(V) cyanoximates were characterized by elemental analysis, thermal analysis, IR-, $^{13}C\{^{1}H\}$ NMR, some with UV-visible spectroscopy, and single crystal X-ray analysis. Eight new crystal structures were determined. All organoantimony(V) cyanoximates demonstrated a pentavalent coordinated distorted trigonal bipyramid polyhedron of the Sb(V) atom. Cyanoxime anionic ligands of each determined structure were bound to Sb(V) in a monodentate fashion. Antimicrobial Disk studies indicated that $Sb(Ph)_4(ACO)$, $Sb(Ph)_4(ECO)$, had significant antimicrobial effect against all three strains: two gram-negative a) *Escherichia coli* strain S17 and b) *Pseudomonas aeruginosa* strain PAO1, alongside a single gram-positive Methicillin-resistant *Staphylococcus aureus* strain NRS70. $Sb(Ph)_4(TCO)$ and $Sb(Ph)_4(TDCO)$ had significant effects on the gram- positive Methicillin-resistant *Staphylococcus aureus* strain NRS70, but essentially no antimicrobial activity for gram-negative strains used. Antimicrobial broth dilution MIC assays were completed against the same strains as antimicrobial disk studies but changed the compounds tested. Using $Sb(Ph)_4(MCO)$ as the only Sb(V) cyanoximate along with the free cyanoximes H(MCO), H(ECO), and $Na[H(ACO)_2]$. Results indicated that free cyanoximes have no antimicrobial effect as the DMSO solvent used in these assays contributed to the inhibition factor to the MIC of the cell cultures. Antifungal disk assays concluded that $Sb(Ph)_4(ECO)$ was effective against *Cryptococcus neoformans* and *Candida albicans* in a positive trend. $Sb(Ph)_4(TCO)$ followed in antifungal activity against both strains. $Sb(Ph)_4(ACO)$ and $Sb(Ph)_4(TDCO)$ were only effective at inhibition of *Cryptococcus neoformans*. Antifungal MIC assays were conducted and concluded that the free cyanoximes had zero effect on antifungal activity against both fungi. On the other hand, $Sb(Ph)_4(MCO)$ had shown MIC levels ranging from 10 - 50 μg/mL.

Before details of the project are given and results briefly described, it is appropriate to provide some important background information about antimony, its basic chemistry and aspects of its biological activity and applications.

Antimony: Chemistry and Applications

Antimony is a ***metalloid*** chemical element with the symbol Sb and an atomic number of 51. Antimony has been known since ancient times and represents shiny silvery solid (Figure 2) resembling metals but much lighter and not conducting electricity. The element "antimony" was named around ~50 AD, where the Roman scholar Pliny gave the name ***stibium***. The original discoverer of antimony is not known, but many people attribute antimony with Nicolas Lemery, a French chemist that performed one of the earliest studies on the element. Other writings attributed to the Arabic father of chemistry Jabir ibn Hayyan used the name *antimonium*. Antimony has the electronic structure [Kr] $4d^{10}\ 5s^2\ 5p^3$ and has readily accessible oxidation states of -3, 0, +3, and +5. The trivalent and pentavalent oxidation states of antimony are the most important as they are found more commonly in nature. There are two stable isotopes of antimony, ^{121}Sb with a natural abundance of 57.36% and ^{123}Sb with a natural abundance of 42.64%. There are also, 35 radioisotopes, with the longest-living isotope being ^{125}Sb with a half-life of 2.75 years. As

antimony is chemically reactive, it forms numerous chemical compounds. Values of various bond energies of electron withdrawing elements with antimony can be found in Table 1. Clearly Sb forms one the strongest bonds with F, O and N atoms. However, natural presence of antimony always is in its compounds with chalcogens and this metalloid often named as oxophilic element.

Figure 2. Actual physical appearance of pure elemental antimony.

Table 1. Bond energies between Sb and halogens, chalcogens and are N - typical ligands in organoantimony compounds.

Sb – E	**E, kcal/mol**
Sb-F	105 ± 23
Sb-Cl	86 ± 12
Sb-Br	75 ± 14
Sb-O	103.7 ± 10
Sb-S	90.5
Sb-Te	66.3 ± 0.9
Sb-N	110 ± 20

Applications of antimony. Antimony can be found naturally as sulphide and oxide ores, which are present in two forms, stibnite (Sb_2S_3) and valentinite (Sb_2O_3). These ores can be found in large quantities in China, South Africa, Mexico, Bolivia, and Chile. Less common sulfide ores include ullmanite (NiSbS), livingstonite ($HgSb_4S_8$), tetrahedrite (Cu_3SbS_3), wolfsbergite ($CuSbS_2$), and jamesonite ($FePb_4Sb_6S_{14}$). One of the traditional treatment methods occurs by roasting stibnite or valentinite ore with charcoal or coke to promote a volatile oxide fume (Sb_4O_6), which can then be refined into pure antimony. During ancient times, stibnite was commonly used for cosmetic purposes in Egypt. The distribution of domestic antimony consumption is estimated as follows:

nonmetal products (including ceramics, glass, and rubber products), 22%; flame retardants, 40%; and metal products, such as antimonial lead and ammunition, 39%.

One of the important uses of antimony metal is as a hardener in lead alloys for storage batteries. Antimony metal has other applications in solders and other metal alloys. Some other uses for antimony alloys include "type metal", which is used in printing presses, bullets, and cable sheathing. Stibine (SbH_3), a gaseous compound used in semiconductor technology, where the purified gas serves as a *n*-type dopant for silicon. One of the most commercially relevant antimony compounds used today is the trivalent antimony trioxide Sb_2O_3. The compound is processed from the metalloid and is used in polyethylene terephthalate and flame-retardant production, and as an additive in paints, pigments, and ceramics. Some flame-retardant applications are used in aircraft and automobile seat covers and children's clothing and toys.

Medicinal applications of antimony. Typical concentration profiles for metal/metalloid ions/atoms in cells are presented in Figure 3 and explain their role in living organisms. The antimony is in between those two.

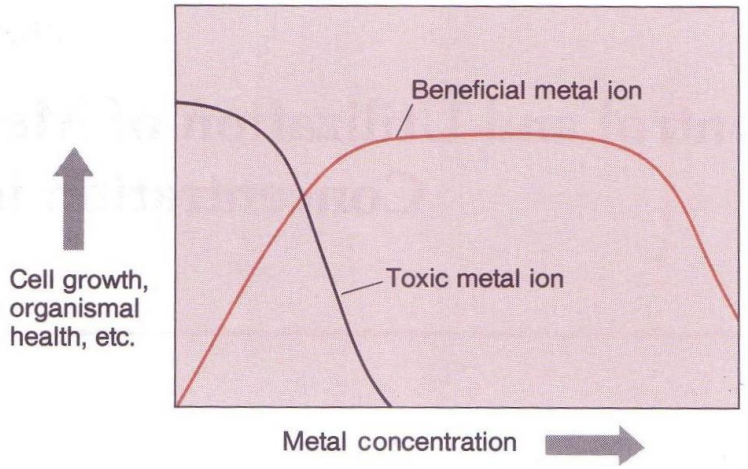

Figure 3. Representation of the concentration dependence of toxic and beneficial effects of metal ions on cell growth.

Thus, organoantimony compounds have shown significant antimicrobial, antitumor, and antifungal activity. Organoantimony compounds also show antitumor activity in some diphenyl-organoantimony(V) thiophosphates such as $Ph_2Sb\{S_2\text{-}PR_2\}$ (Ph = C_6H_5, R = Ph, *i*-OC_3H_7) and methylantimony(III) complexes like $(CH_3)SbL$ (L = derivatives of meta-substituted salicylic acid. Due to similarity of the mechanism, cytostatic activity is attributed to these complexes, which is correlative to cisplatin. Furthermore, the biological toxicity of organoantimony is much less than that of Pt and Pd in the case of anticancer substances. In addition, antimony compounds have been used in treatment against the parasitic disease leishmaniasis for about a century.

Leishmaniases is caused by the protozoan parasite under the genus *Leishmania* which then multiplies in certain vertebrates. The parasite is transmitted to humans through the bite of sandflies that are infected. Multiple forms of the disease exist; the two most known are cutaneous leishmaniasis (CL) the most common form and visceral leishmaniasis (VL) the most severe. The earliest treatment reported of CL used a trivalent antimonial, tartar emetic, in 1913. Over a decade after the report, tartar emetic was criticized as an antimonial due to side effects such as heavy coughing, chest pain, and severe depression. In addition, the compound was found to be very unstable in a tropical climate and highly toxic. The disadvantages posed by trivalent antimonials lead to the discovery of treatment with pentavalent antimonials. These included urea stibamine, antimony gluconate, and sodium stibogluconate. Currently, the most commonly used organoantimony compounds against leishmaniasis are the pentavalent sodium antimony gluconate (Pentostam) and meglumine antimoniate (Glucantime).

The most accepted, proposed mechanism of pentavalent antimonial is their behavior as prodrugs. The pentavalent prodrug undergoes *in vivo* biological reduction into a much more active/toxic trivalent antimony. This Sb^{5+} to Sb^{3+} reduction requires thiol compounds of both mammalian and parasitic origin. Mammalian thiols include glutathione (GSH), cysteine (Cys), and cysteinyl-glycine (Cys-Gly). Glutathione is the main thiol in the cytosol, while cysteine and cysteinyl-glycine are the predominant thiols within lysosomes of mammalian cells. The parasitic thiol compound required is trypanothione ($T(SH)_2$), this complex consists of glutathione and spermidine. Intake of pentavalent antimony into parasitic cells has been suggested to occur by monoadduct formation between Sb^{5+} and nucleotides. This can be attributed to nucleotides containing vicinal *cis*-hydroxyl groups (i.e. adenosine, cytidine, guanosine, uridine, and AMP), where binding occurs at the deprotonated hydroxyl group of the ribose moiety. The complexation leads to nucleotides acting as carriers for Sb^{5+} into parasites via lipophospholycan (LPG) transporter. Figure 4 represents the intake of metal compounds and ions into the cell either through passive diffusion or an ion specific channel. Once inside the parasitic cell, the application of a prodrug can proceed. The reduction can occur enzymatically (through ACR2 or TDR1 reductase) or non-enzymatically. Once the reduction has occurred complexation between glutathione or trypanothione.

The first site of interference is with the trypanothione/TR system. This system maintains trypanothione in the reduced state to balance the oxidoreductive balance in the *Leishmania* parasite. This balance protects the cell from oxidative stress damage, toxic heavy metals, and delivers reducing power for DNA synthesis. Trivalent antimonials interfere with trypanothione metabolism by inhibiting trypanothione reductase (TR) and inducing rapid efflux of intracellular trypanothione and glutathione into unaffected *Leishmania cells* which lead to apoptosis. The second site of attack by trivalent antimony is with the CCHC zinc finger domain. Zinc fingers can be characterized by the coordination of zinc with several amino acid residues, typically cysteine
and histidine. This domain has purpose in a variety of diverse functions such as DNA recognition and replication and structure and repair, RNA packing, protein folding and assembly, lipid binding, transcriptional activation, cell differentiation, cell growth, and regulation of apoptosis. Once

trivalent antimony is bound to the zinc finger domain, promotion of efflux of Zn^{2+} occurs, leading to apoptosis. Figure 5 illustrates the prodrug model.

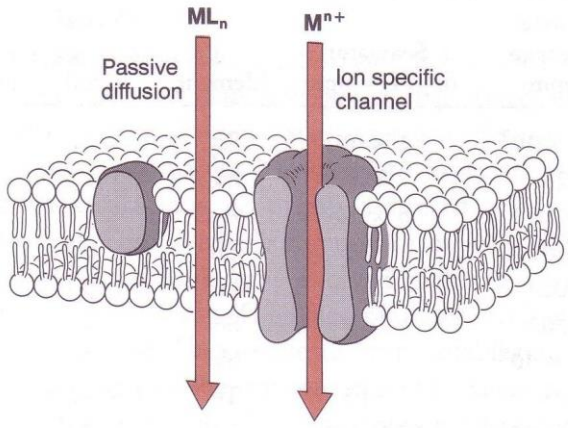

Figure 4. Schematic representation of how chemical compounds enter the cell, taken from literature.

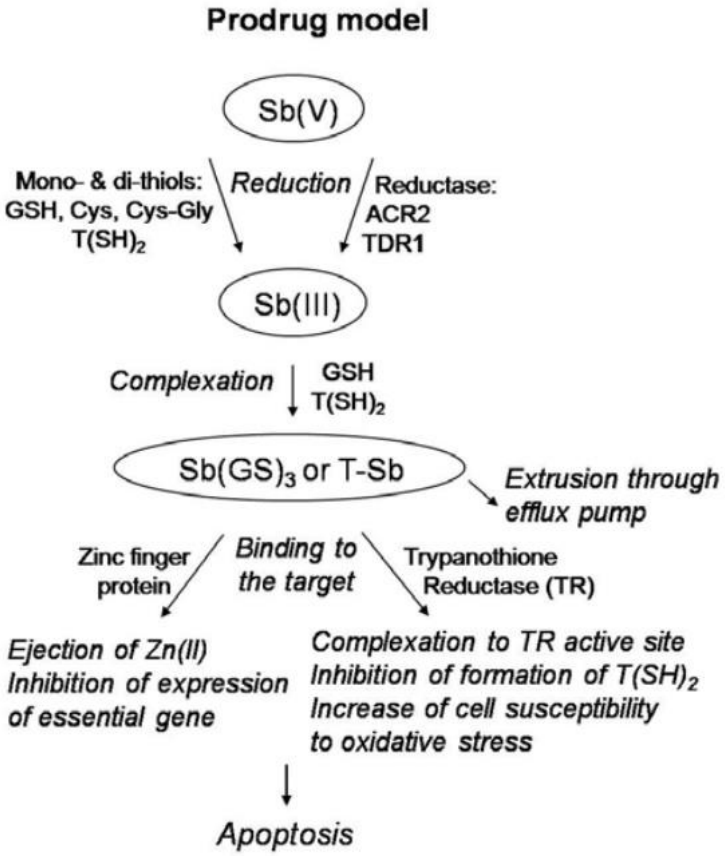

Figure 5. Model of pentavalent antimonials as prodrugs taken from literature.

Synthesis of organoantimony(V) compounds.

We found experimentally in the past that the best method of preparation of organoelemental derivatives of pseudohalides and cyanoximes is metathesis reaction, which is in essence a "double displacement" with the formation of insoluble in water and common organic solvents silver(I) or thallium(I) halides. It is a clean, heterogeneous reaction in which desired product of such exchange stays in solution and can be easily separated from insoluble the above salts by filtration or centrifugation. In that way we made series of organotin(IV), organotellurium(IV) and organoantimony(V) derivatives.

Employed in this research project reaction utilizing light stable either silver(I) cyanoximates is shown in Figure 6. Unfortunately, not all planned for such double displacement reactions Ag(I) cyanoximates are stable and convenient for handling. More specifically, thioamide-cyanoximes TCO and TDCO (see Figure 1) do not form Ag(I) salts and any attempts to make them result in black Ag_2S. Therefore, we had to use their Tl(I) salts which is shown in Figure 7.

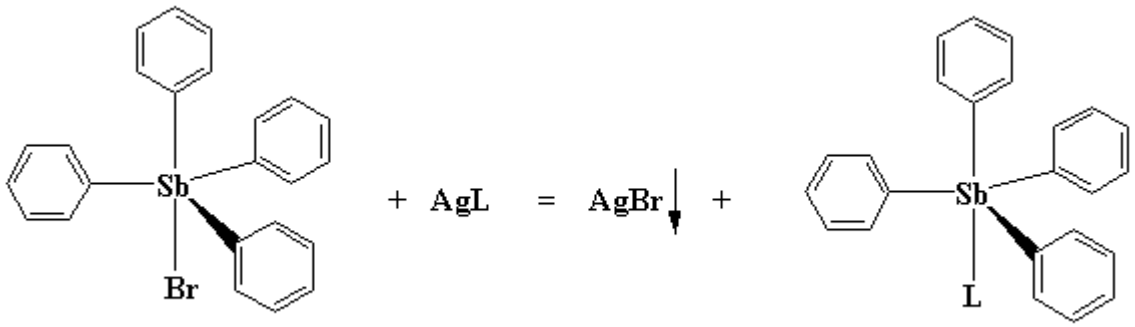

Figure 6. General synthesis of organoantimony(V) cyanoximates using the metathesis reaction with silver(I) salts. L represents the variety of ligands chosen for study.

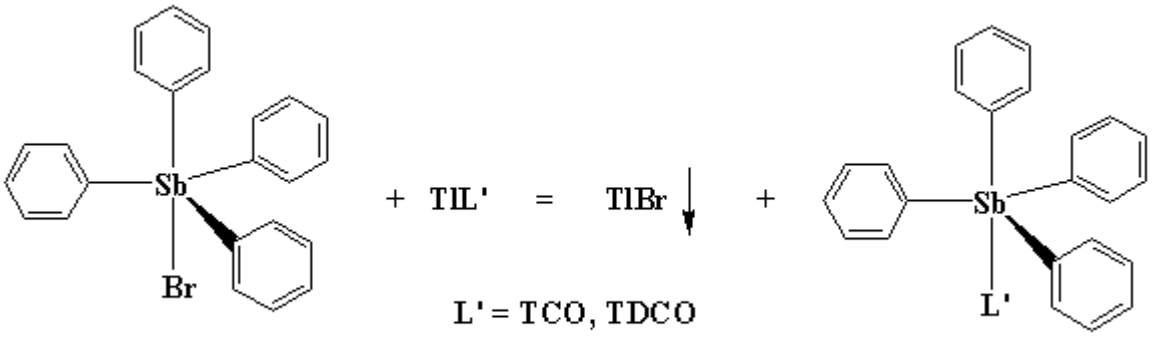

Figure 7. General synthesis of organoantimony(V) cyanoximates using the metathesis reaction with thallium(I) salts. L' represents the thioamide containing ligands.

All prepared Sb(V) cyanoximates represent either crystalline or powdery substances well soluble in organic solvents. Actual appearance of some compounds is shown in Figure 8.

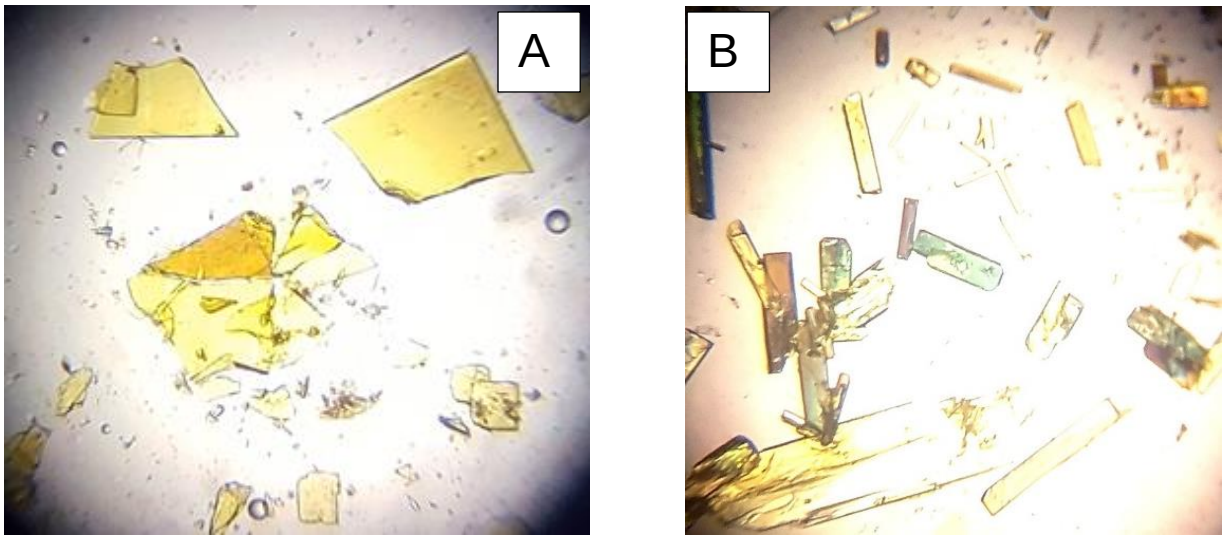

Figure 8. Microscope taken image of desired crystalline organoantimony(V) cyanoximate, $SbPh_4$(TDCO) (**A**), and $SbPh_4$(TCO) (**B**).

Characterization of synthesis of organoantimony(V) compounds.

All 8 synthesized new tetraphenylantimony(V) cyanoximates were studied using thermal analysis (TG/DSC method), vibrational, UV-visible and ^{1}H, ^{13}C NMR spectroscopy. Yields of preparations and data of chemical content determination for all obtained in Kevin's work compounds are summarized in Table 2 below.

Some selected thermal analyses traces are presented in Figure 9 and Figure 10 and in Table 3 and show considerable thermal stability of the obtained $SbPh_4L$ compounds up to 160^{o}C, which is important for their intended practical application as antimicrobial agents. Thus, method was used to aseess compounds' thermal stability and determine accurate phase transitions. The DSC-TGA analysis of the Sb(V) cyanoximates are described Table 3. A typical thermogram of the $SbPh_4$(ECO) monomer shows an endothermic peak of heat flow at 144.7°C representing and endothermic effect due to melting point (Figure 9).

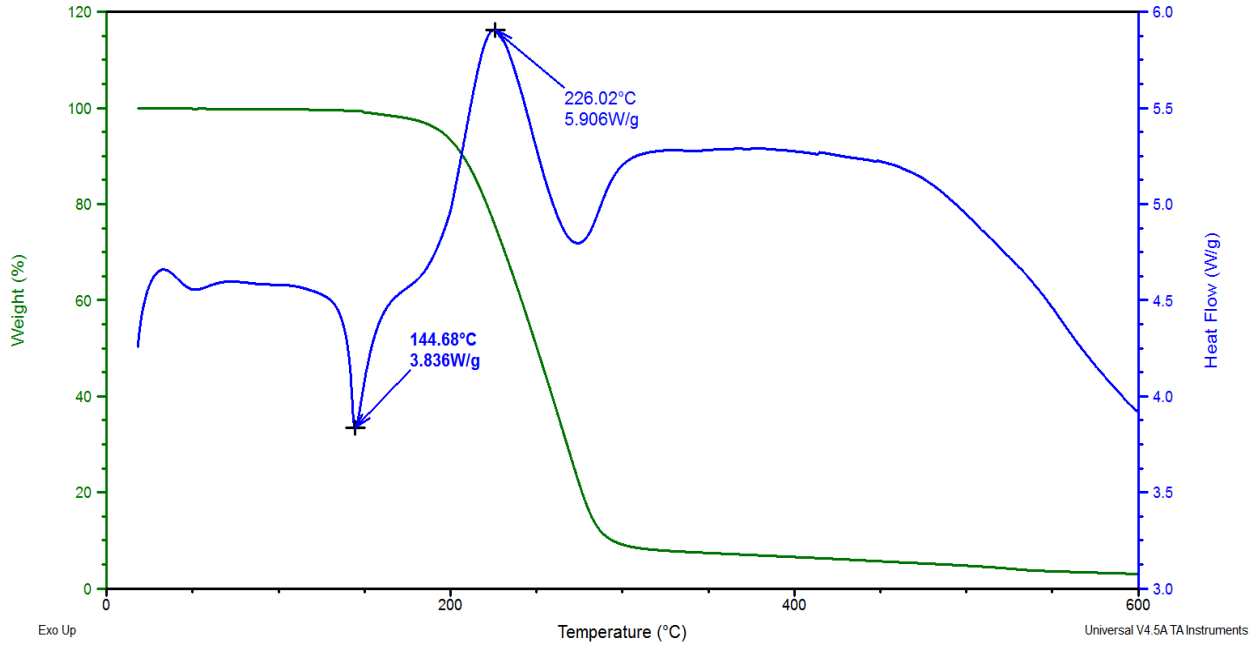

Figure 9. Traces of weight loss (green) and heat flow (blue for the $Sb(Ph)_4(ECO)$ monomer showing the melting point of the compound at 144°C followed by its decomposition at ~220^{o}C.

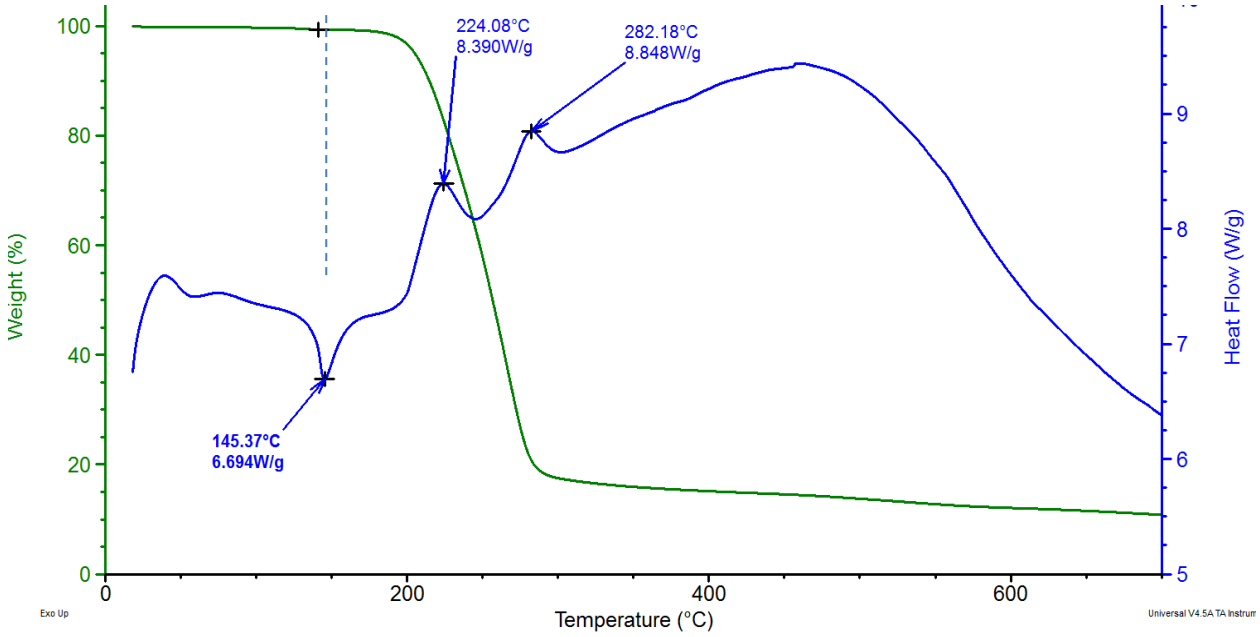

Figure 10. TG/DSC traces for a sample of $SbPh_4(4PCO)$ showing compounds melting followed by decomposition after ~160^{o}C.

Table 2. Color, yield, and elemental analysis of synthesized organoantimony(V) cyanoximates and their precursors.

Compound	Color	Yield (%)	Elemental analysis, element %			
			C, % Calc. (Found)	H, % Calc. (Found)	N, % Calc. (Found)	S, % Calc. (Found)
pre-MCO	white	65	-	-	-	-
HMCO	off-white	82	-	-	-	-
Ag(MCO)	yellow		28.99 (28.19)	2.78 (2.81)	14.49 (14.06)	-
$Sb(Ph)_4(MCO)$	colorless	90	60.81 (59.48)	4.61 (4.52)	8.86 (6.47)	-
$Sb(Ph)_4(2PCO)\cdot H_2O$	colorless	45	64.61 (64.34)	4.20 (4.07)	7.29 (7.19)	-
$Sb(Ph)_4(3PCO)$	colorless	84	64.61 (62.17)	4.20 (3.99)	7.29 (6.51)	-
$Sb(Ph)_4(4PCO)$	colorless	46	64.61 (63.93)	4.20 (3.93)	7.29 (7.31)	-
$Sb(Ph)_4(ACO)$	colorless	79	59.81 (58.39)	4.09 (4.16)	7.75 (7.29)	-
$Sb(Ph)_4(ECO)$	colorless	91	60.86 (60.59)	4.58 (4.44)	4.89 (4.94)	-
$Sb(Ph)_4(TDCO)$	golden yellow	51	59.40 (58.84)	4.47 (4.37)	7.17 (6.20)	5.47 (4.64)
Tl(TCO)	yellow		10.84 (10.77)	0.61 (0.54)	12.64 (12.71)	9.64 (9.52)
$Sb(Ph)_4(TCO)$	yellow	51	58.08 (57.93	3.97 (3.84)	7.53 (7.42)	5.74 (5.59)

Table 3. Results of thermal analysis studies of organoantimony(V) cyanoximates.

Compound	Events, temperatures (ºC)
$SbPh_4(2PCO)\cdot H_2O$* weight loss for ~1 H_2O at ~166	*endo*-, melting at 204.2; decomposition, *exo*- at 249
$SbPh_4(3PCO)$	*endo*-, melting at 146.9; decomposition, *exo*- at 199
$SbPh_4(4PCO)$	*endo*-, melting at 145.4; decomposition, *exo*- at 224 and second decomposition, *exo*- at 283
$SbPh_4(ACO)$	*endo*-, melting at 199.5; decomposition, *exo*- at 239
$SbPh_4(ECO)$	*endo*-, melting at 144.7; decomposition, *exo*- at 226
$SbPh_4(MCO)$	*endo*-, melting at 175.2; decomposition, *exo*- at 238
$SbPh_4(TCO)$	*endo*-, melting at 185.6; decomposition, *endo*- at 239; and second decomposition, *endo*- at 286
$SbPh_4(TDCO)$	*endo*-, melting at 148.7; decomposition, *exo*- at 221

*- X-ray structure gives evidence of anhydrous behavior. Therefore, the complex most likely absorbed moisture from handling.

We were fortunate to be able to crystallize these eight novel compounds and determine their crystal and molecular structures which will be displayed below in Figures 11 – 26 together with some explanations and comments. In all compounds trigonal bipyramid SbC4O environment was found.

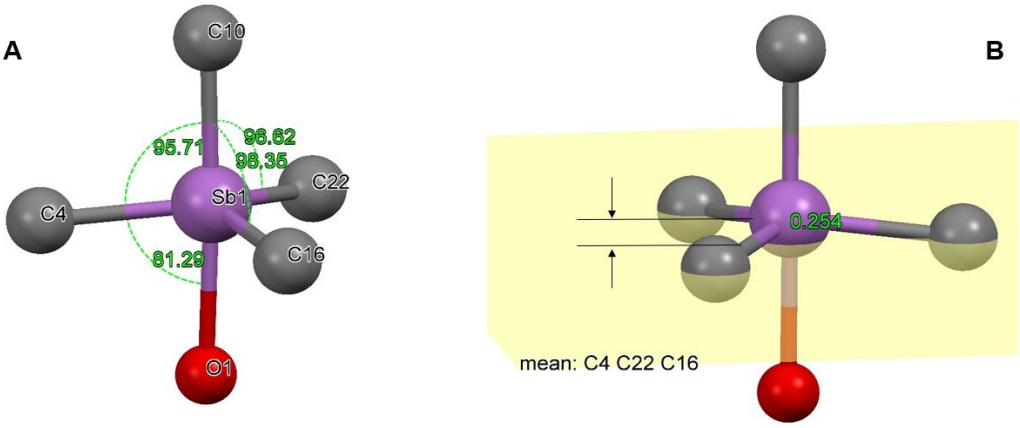

Figure 11. A, analysis of the angles of the coordination polyhedron of Sb(V) in $SbPh_4(ACO)$. **B**, analysis of planarity between Sb(V) core and equatorial *ipso* carbons of the phenyl rings.

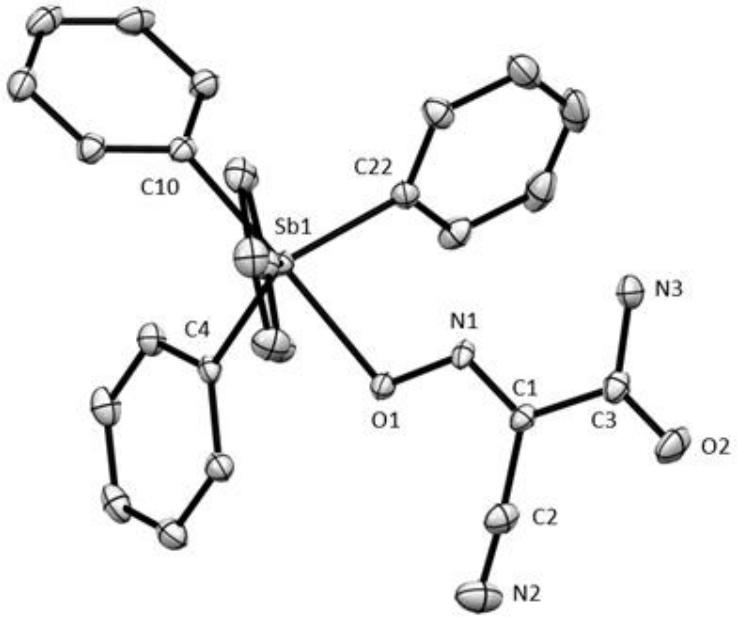

Figure 12. Molecular structure and numbering scheme of principal atoms in the crystal structure of $SbPh_4(ACO)$. An ORTEP representation at 50% thermal ellipsoid probability. H-atoms omitted for clarity.

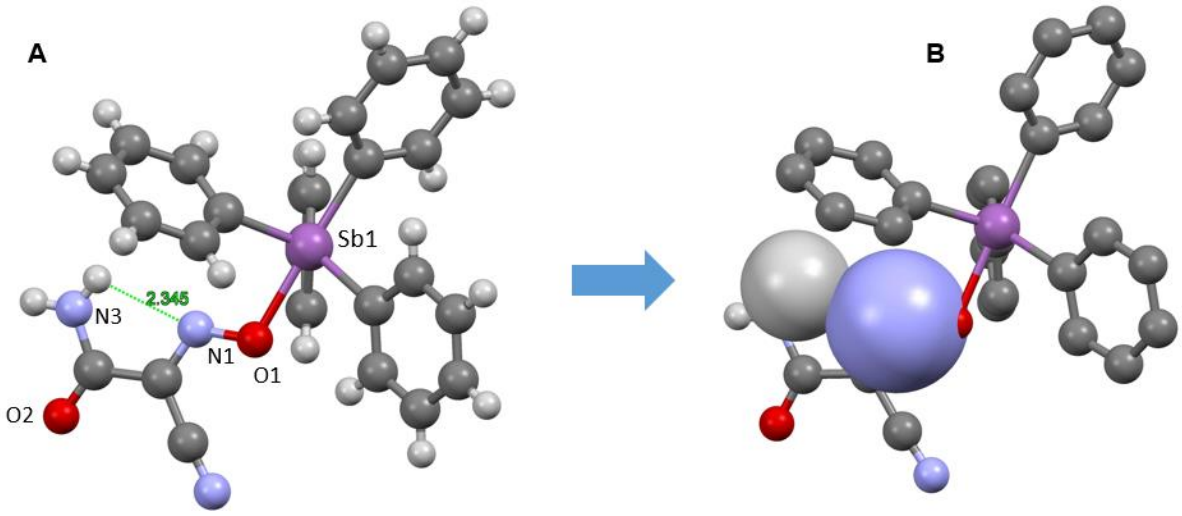

Figure 13. Two least obstructed views of $SbPh_4(ACO)$ showing structure stabilization through intramolecular H-bonding of H1a and N1, **A**, along with the space filling model , **B**.

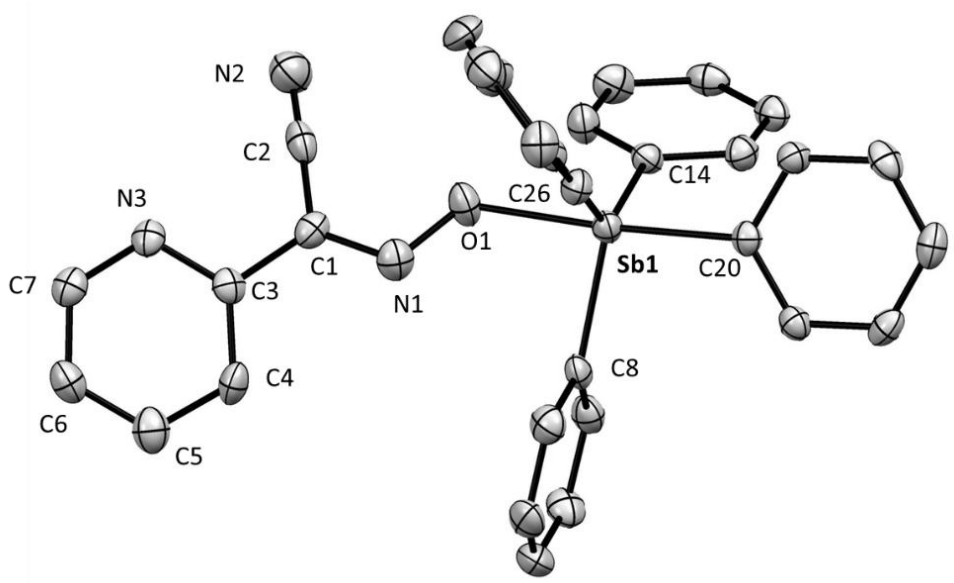

Figure 14. An ORTEP drawing at 50% thermal ellipsoids probability level for the ASU $SbPh_4(2PCO)$ showing the numbering of principal atoms. H-atoms are omitted for clarity.

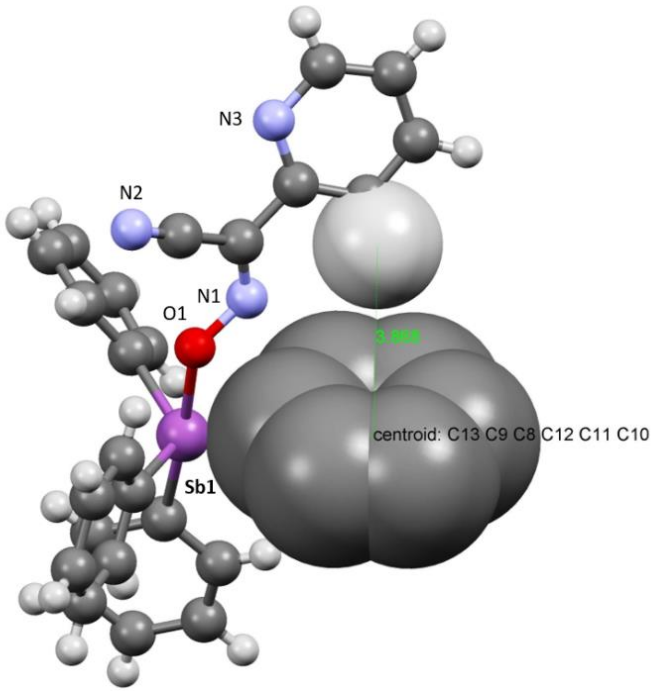

Figure 15. Structure of intramolecular stabilization through electrostatic contact of equatorial phenyl ring π-system and pyridyl hydrogen of $SbPh_4(2PCO)$. Involved atoms are expressed in a space-filling mode.

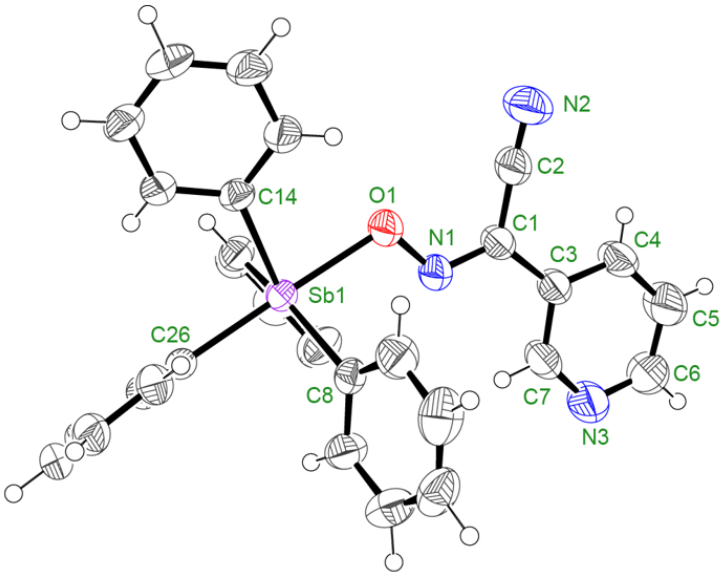

Figure 16. An ORTEP drawing at 50% thermal ellipsoids probability level for the ASU $SbPh_4(3PCO)$ showing the numbering of principal atoms.

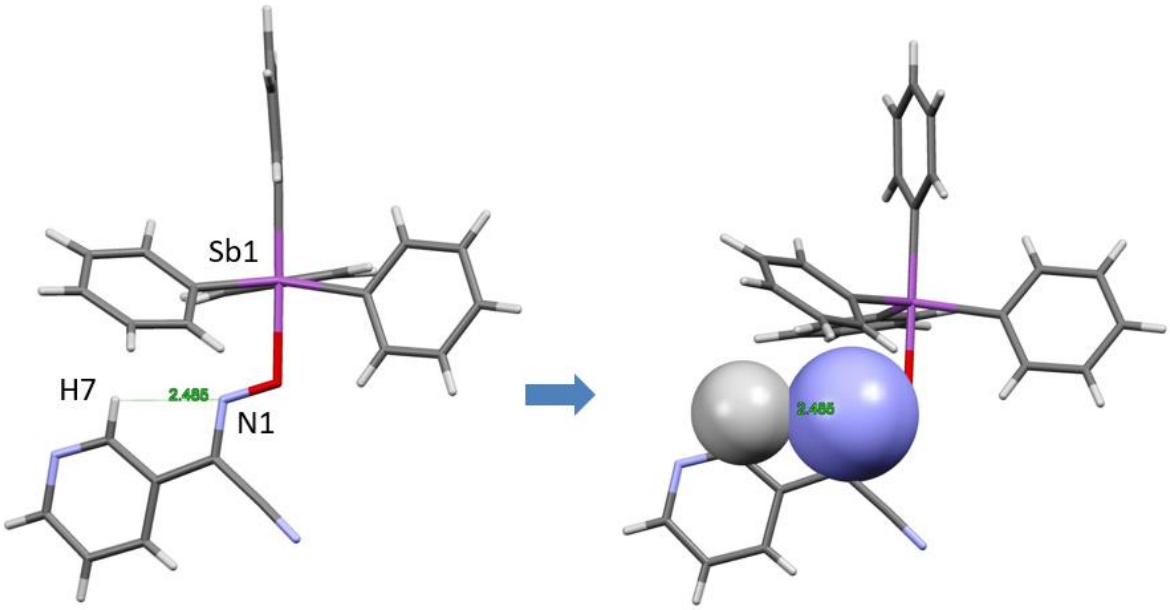

Figure 17. The least obstructed view of the ASU of $SbPh_4(3PCO)$ showing intramolecular electrostatic contact of the pyridyl hydrogen (H7) with the nitrogen (N1) of the cyanoxime's moiety.

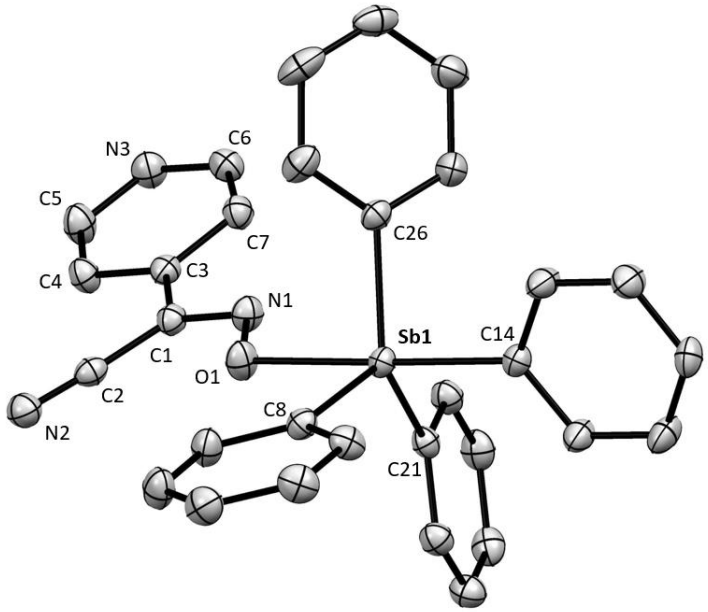

Figure 19. An ORTEP drawing at 50% thermal ellipsoids probability level for the ASU $SbPh_4(4PCO)$ showing the numbering of principal atoms. H-atoms are omitted for clarity.

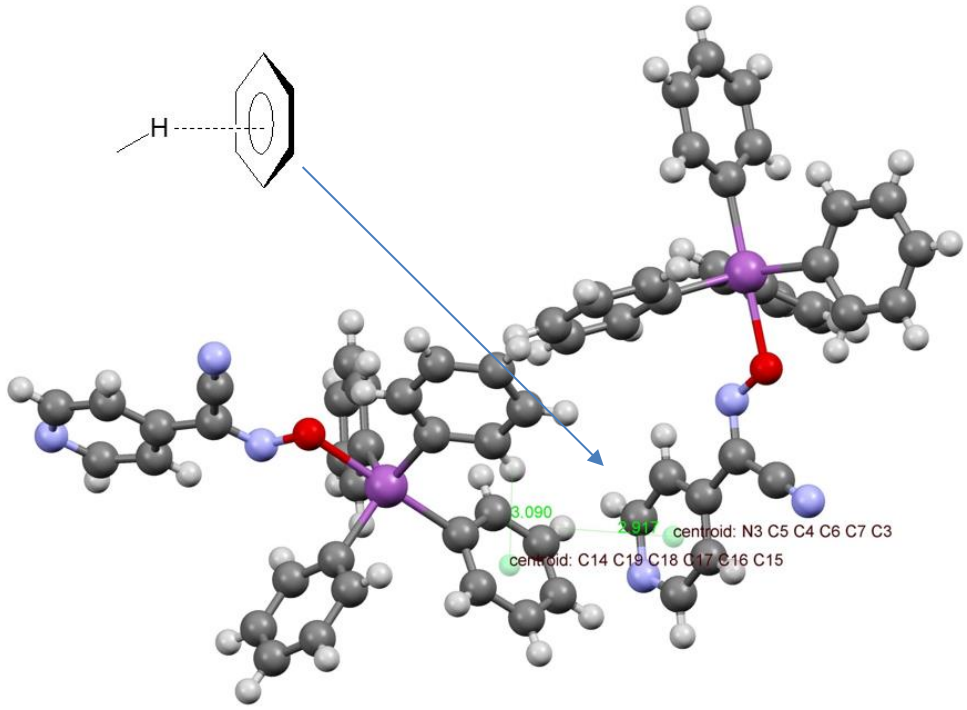

Figure 20. Packing of two structures of $SbPh_4(4PCO)$ showing stabilization short electrostatic contact between the centers of the 4-pyridyl centroid and phenyl rings with phenyl hydrogens.

Kevin experimentally found that when water was added into the reaction mixture, not monomeric, but rather dimeric compound with bridging oxygen atom was formed! Its structure is shown in Figure 21 with tentative mechanism of such dimerization displayed in Figure 22. In involves two step processes: hydrolysis and then dimerization. The last step took place when Kevin heated to ~50^{o}C the reaction mixture. This type of behavior was normally observed in transition metals complexes with planar aromatic systems such porphyrins, phtalocyanins and texaphyrins. Thus, to the best of our knowledge this is the first fact of dimerization with the formation of Sb-O-Sb linear fragment with 180^{o} angle!

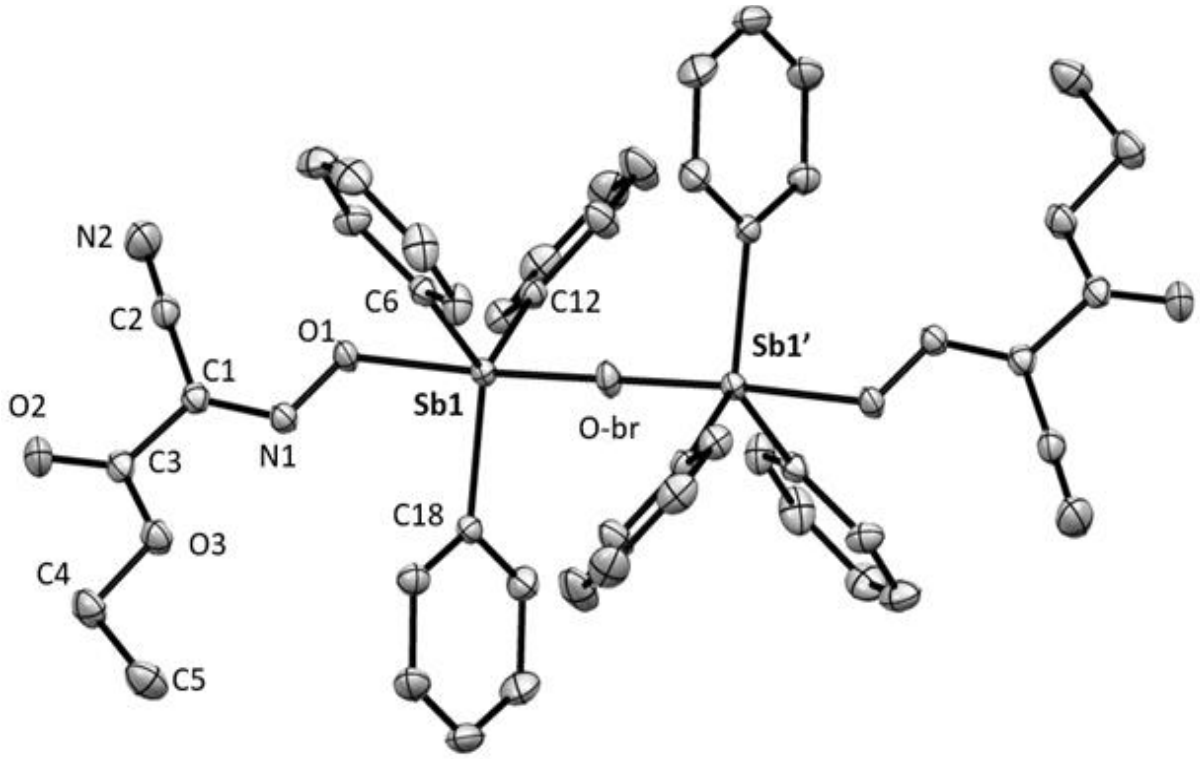

Figure 21. An ORTEP drawing at 50% thermal ellipsoids probability level for the ASU in the structure of $SbPh_3(ECO)$ μ-oxo-dimer showing the numbering of principal atoms. H-atoms are omitted for clarity.

In strictly controlled anaerobic conditions real monomeric compound of $SbPh_4(ECO)$ was obtained and its structure presented in Figure 23. Surprisingly, there were two crystallographically independent molecules observed in the asymmetric unit (ASU) of the structure. Another peculiarity is non-centrosymmetric space group Pn for crystallization of monomeric compound. Similar story with crystallization of two independent molecules in one ASU of the unit cell happened in case of SbPh4(MCO) compound structure of which is described in Figure 24 below.

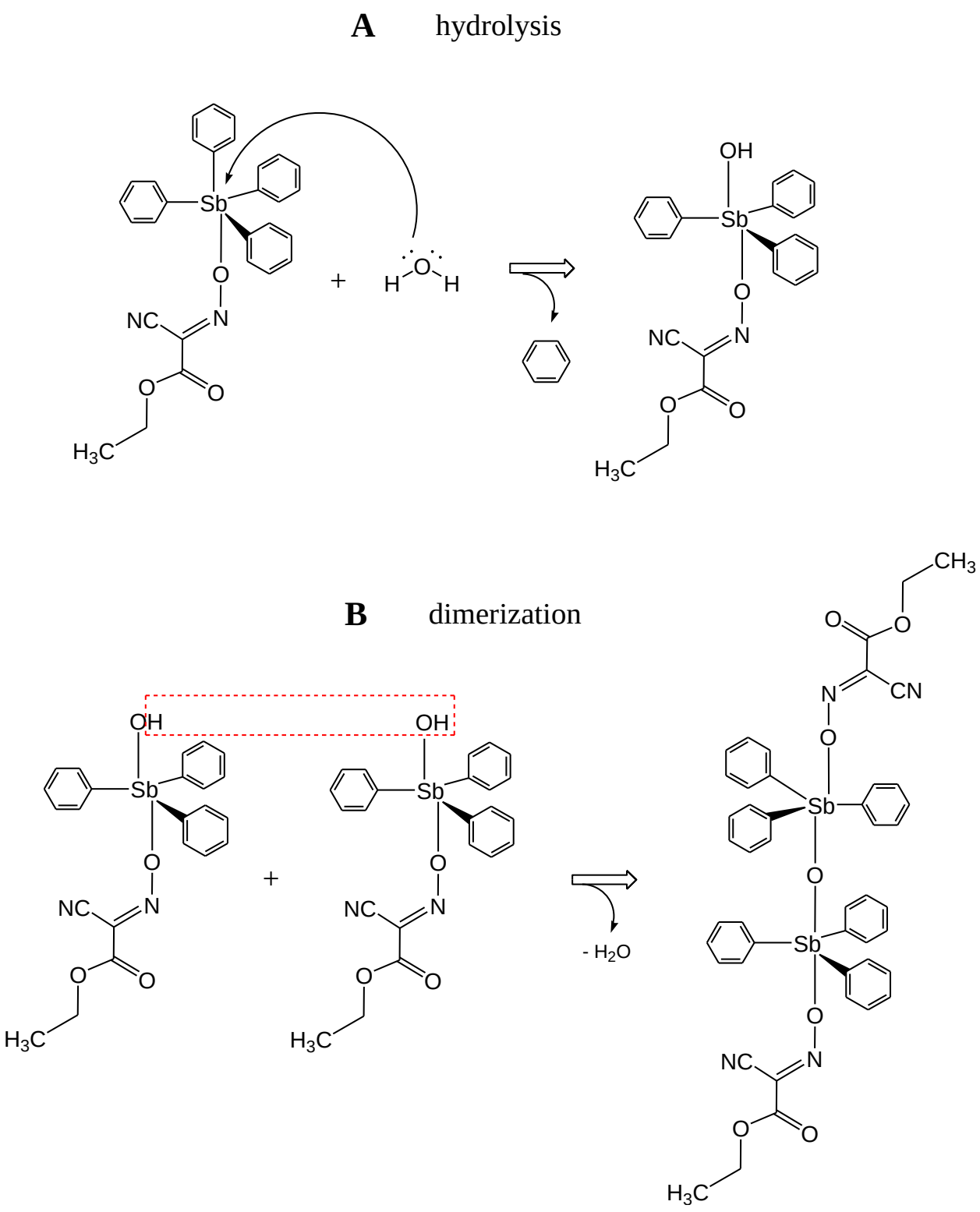

Figure 22. Scheme of suggested path for hydrolysis, **A**, and the dimerization, **B**, of organoantimony(V) in moist conditions.

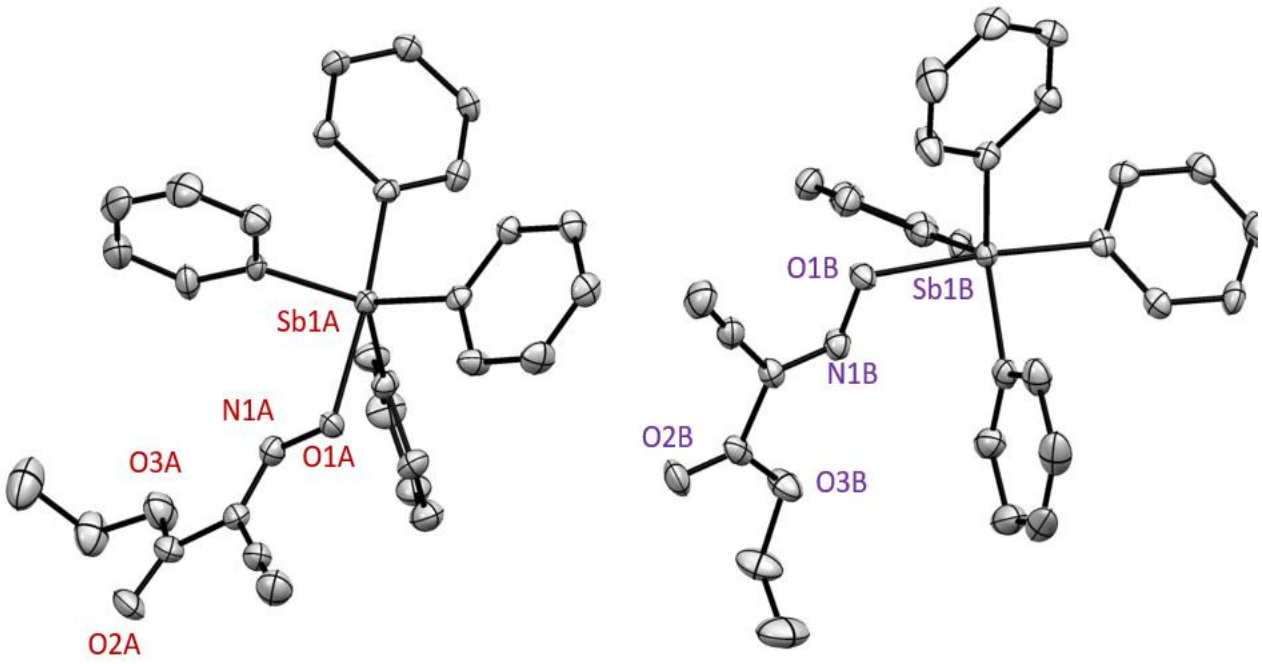

Figure 23. An ORTEP drawing at 50% thermal ellipsoids probability level for the two crystallographically independent molecules in the ASU of $SbPh_4(ECO)$ monomer showing the numbering of principal atoms. H-atoms are omitted for clarity.

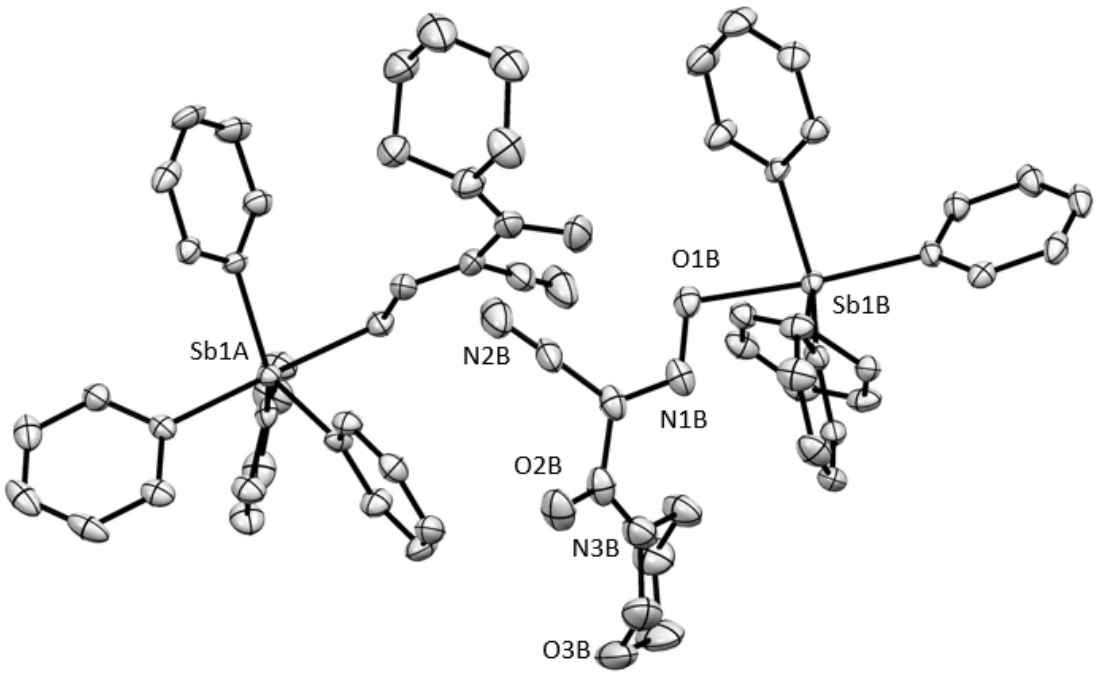

Figure 24. Two independent molecules in the ASU of the structure of $SbPh_4(MCO)$; and ORTEP drawing at 50% thermal ellipsoids probability level. Principal only atoms are labeled, with H atoms being omitted for clarity.

Another peculiarity found during Kevin's work on the project was observation of co-crystallization of two diastereomers in the same unit cell. That is *syn*- and *anti*- forms of the cyanoxime were binding to the Sb center via O-atom, but overall geometry of the anion was quite different as explained in Figures 25 and 26.

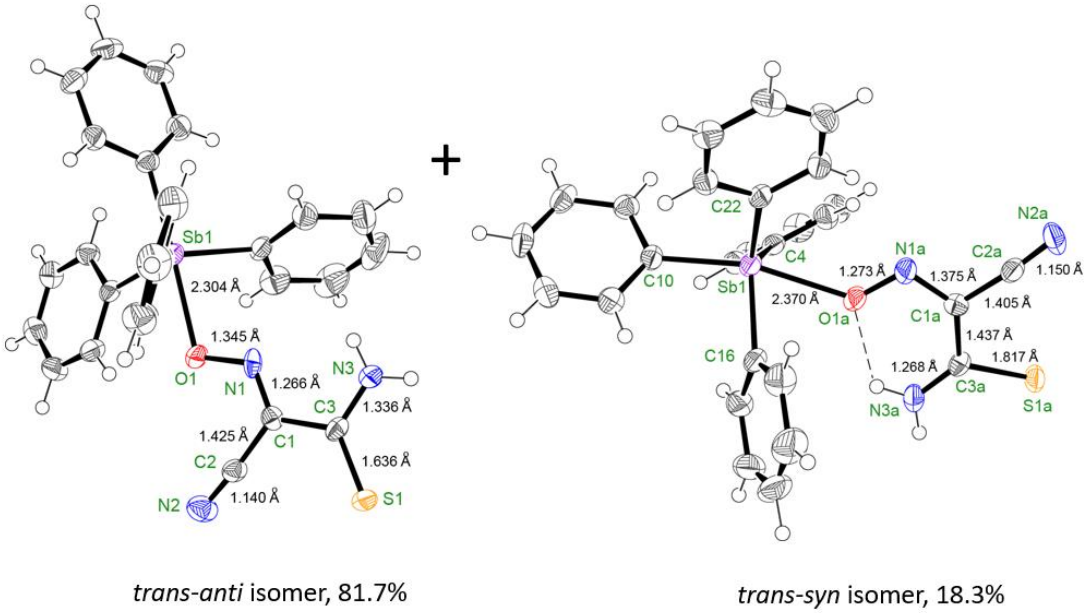

trans-anti isomer, 81.7%

trans-syn isomer, 18.3%

Figure 25. Two least obstructed views of the two diastereomers of $Sb(Ph)_4(TCO)$ in the ASU representing H bonding stability between the amide hydrogen (N-H3a) and O1a. Ratios of two diastereomers are shown.

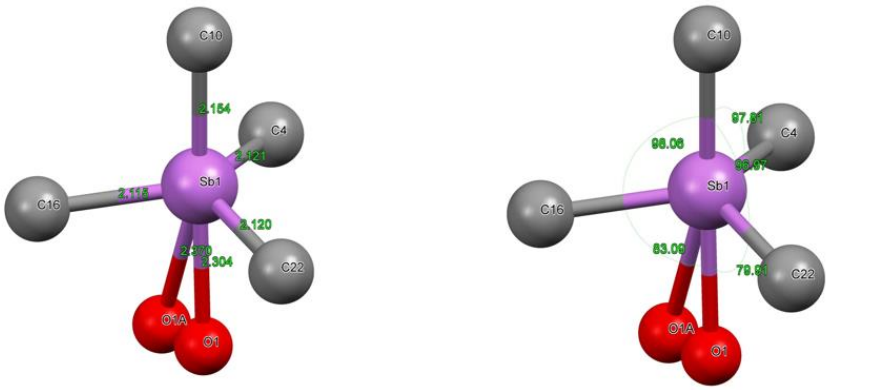

bonds

angles

angles C10-Sb1-O1 = 176.86°
C10-Sb1-O1a = 164.12°

Figure 26. Geometry of the pentavalent antimony complex $Sb(Ph)_4(TCO)$ diastereomers, showing a distorted trigonal bipyramid polyhedron coordination. Important bond lengths and angles of coordination are shown.

Biological studies were conducted at collaborative institution – Oklahoma State University, Stillwater. Two laboratories led by Prof. Marianna Patrauchan and Professor Karen Wozniak carried out this part of investigations of this series of new tetraphenylantimony(V) cyanoximates. Main results of this work as antimicrobial and antifungal studies are shown in Figures 27 - 32.

First set of inhibition measurements on solid media. Initial compounds selected for susceptibility tests were: $Sb(Ph)_4$(ACO), $Sb(Ph)_4$(ECO) monomer, $Sb(Ph)_4$(TCO), and $Sb(Ph)_4$(TDCO). These compounds were tested against gram-negative strains *Escherichia coli* strain S17 and *Pseudomonas aeruginosa* strain PAO1, alongside gram-positive Methicillin-resistant *Staphylococcus aureus* strain NRS70. In this initial test, zone inhibition measurements for $Sb(Ph)_4$(TDCO) were omitted as the PBS buffer was contaminated, results for this compounds were completed in the following round of testing. Figures 54-56 represent the first triplicate set of inhibition zone measurements for antimicrobial activity determination. In the case of $Sb(Ph)_4$(ACO), it showed a trend against all strains of increased clearance zone inhibition as Sb(V) cyanoximate concentration increased (Figure 54). This can be said for the $Sb(Ph)_4$(ECO) monomer for *S. aureus* and *E .coli*, but did not keep that trend against *P. aeruginosa*. Finally, $Sb(Ph)_4$(TCO) demonstrated the decent inhibition against *S. aureus*, but no inhibition at all against *P. aeruginosa* and *E. coli*. Full worksheets including statistical analysis of the first round of susceptibility tests can be found in Appendix D-1 to D-3.

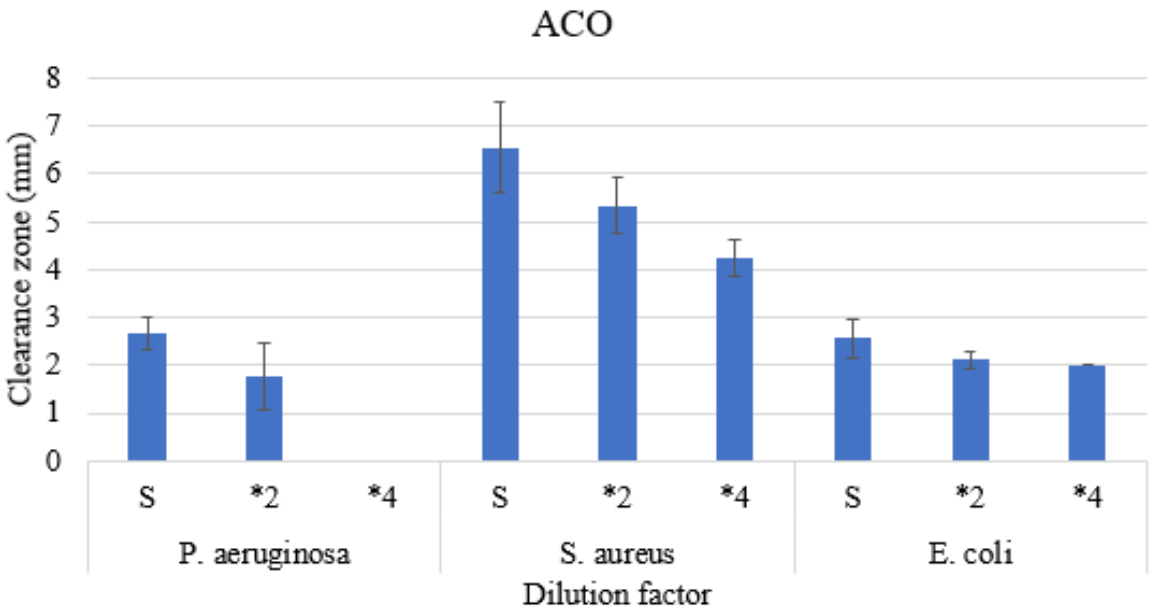

Figure 27. Round 1 of Inhibition zone measurements of $Sb(Ph)_4$(ACO) against microbes.

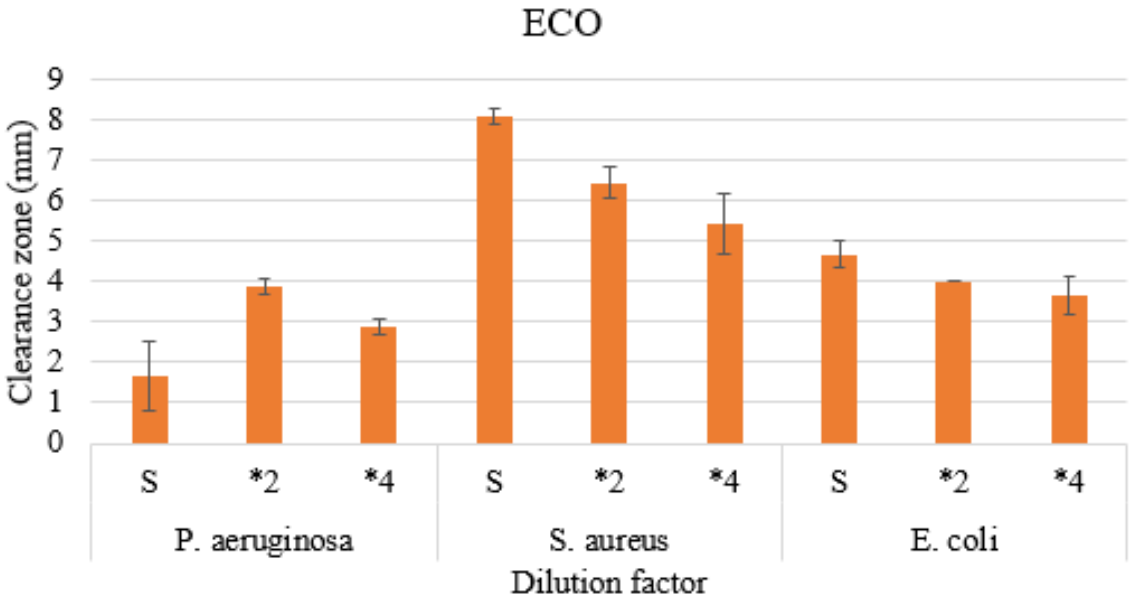

Figure 28. Round 1 of Inhibition zone measurements of $Sb(Ph)_4$(ECO) against microbes.

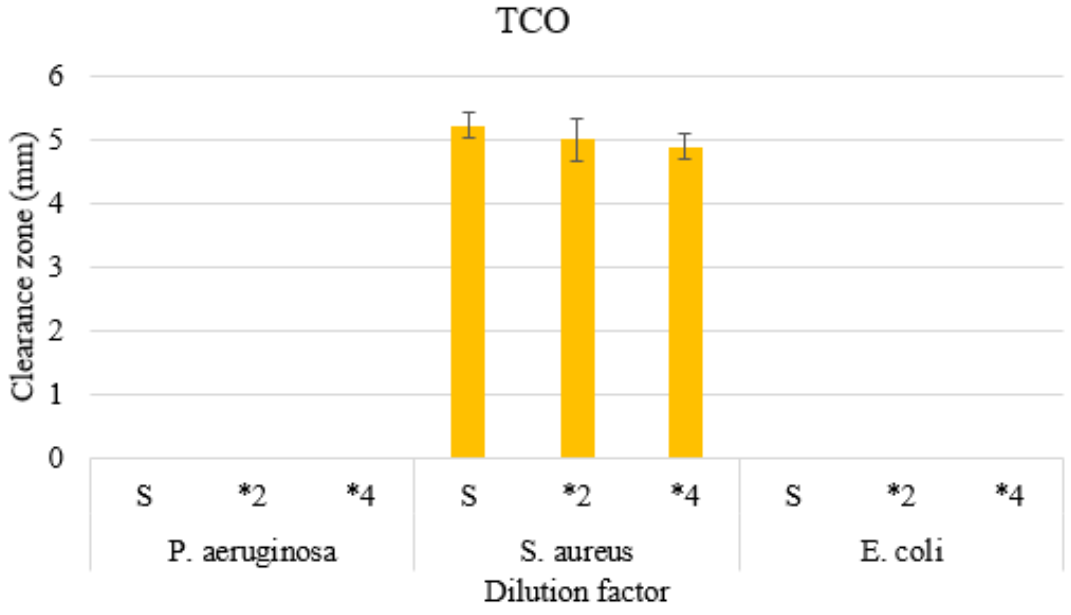

Figure 29. Round 1 of inhibition zone measurements of $Sb(Ph)_4$(TCO) against microbes.

Second set of inhibition measurements. The second round of susceptibility tests added a new compound, a control Sb(Ph)Br (labeled as CC# in Figure 57), and restarted measurements with $Sb(Ph)_4$(TDCO) due to previous contamination of PBS in the experiment. Each were run in triplicate at three different concentrations. The measurements can be found in Figure 57. Essentially the same outcome occurred for $Sb(Ph)_4$(ACO), $Sb(Ph)_4$(ECO), and $Sb(Ph)_4$(TCO) as the first round of tests. For $Sb(Ph)_4Br$ there was no inhibition against *P. aeruginosa*, and some inhibition against *E. coli*.. An interesting outcome is the inhibition zone of $Sb(Ph)_4Br$ with respect to *S. aureus*. A possible reason for this outcome could be due to an ionic halogen exposure to gram-positive bacteria which has less intrinsic defenses as gram-positive bacteria lack a second cell membrane. A similar result with the first round, both of the thioamide cyanoximates, $Sb(Ph)_4$(TCO) and $Sb(Ph)_4$(TDCO), only had antimicrobial effect against the gram-positive *S. aureus* . The result of zone inhibition being present in only the gram-positive *S. aureus* might show that there an instrinsic antimicrobial resistance against thioamide-containing organoantimony cyanoximates, though more testing needs to be conducted. Raw data and statistical analysis of this data can be found in under Appendix D-4

Initial broth dilution MIC tests. Initial compounds selected for antimicrobial MIC tests were: $Sb(Ph)_4$(MCO), H(MCO), H(ECO), and $Na[H(ACO)_2]$. The goal of this testing was to determine if free cyanoximes had any effect on inhibition cell growth of the same strains tested in the inhibition zone measurements, as well as testing out an organoantimony(V) cyanoximate. As these compounds were dissolved in DMSO, it must be reiterated that the organic solvent has inhibition effects already once concentrations reach above 5% (Appendix D-1). This inhibition concentration with DMSO would require 200 μg/mL for *P. aeruginosa* and 250 μg/mL for both *E. coli* and *S. aureus.*

Results of the antimicrobial MIC assays are shown in Figure 58 and 59. It is evident in MIC at both the 6 and 24 hours marks that $Sb(Ph)_4$(MCO) had inhibition of cell growth before the DMSO inhibition level at 5%. $Sb(Ph)_4$(MCO) had a definite antimicrobial effect on *E. coli* and *S. aureus* at 200 μg/mL concentration. Compared with *P. aeruginosa*, some inhibition was seen once concentration was increased. Switching over to the free cyanoximes, the inhibition of cells was clearly due to DMSO concentration increasing as the interval from switching to a concentration of zero to 100 μg/mL demonstrated negligible decrease of OD600, therefore an indirect method to quantify microbe concentration. What is a significant factor to free cyanoximes not contributing towards antimicrobial activity is at 6 hours for *P. aeruginosa* for all protonated ligands is the *increase* of concentration from zero to 100 μg/mL causing an increase of microbe concentration. Free cyanoximes tested had no effect against the strain PAO1 of *P. aeruginosa*. As for the other strains, the increasing free cyanoxime concentration had little to no effect on inhibition of microbe growth.

Antifungal Studies. These assays were performed by Dr. Karen Wozinak and her research group. Sample preparation was exactly the same as MIC and susceptibility assays for

antimicrobial studies. Inhibition zone measurements were completed in two parts and both will be discussed, along with reconstituted MIC assays.

Kirby-Bauer disk assays. Initial antifungal studies tested a control (blank cotton disk), $Sb(Ph)_4$(ECO), $Sb(Ph)_4$(ACO), $Sb(Ph)_4$(TCO), and $Sb(Ph)_4$(TDCO) against two strains of fungi: *Cryptococcus neoformans* and *Candida albicans*. Disks were prepared at three different concentrations and run in triplicate. Antifungal disk assays can be seen in Figure 60. A general trend with $Sb(Ph)_4$(ACO), $Sb(Ph)_4$(ECO), $Sb(Ph)_4$(TDCO) against *Cryptococcus neoformans* is that increasing concentration has a positive effect of increasing size of inhibition zone, though for $Sb(Ph)_4$(TDCO), the zone of inhibition was lower at all concentrations when compared to $Sb(Ph)_4$(TCO) which had an opposite trend than the previous three compounds. With regard to *Candida albicans* against our copounds, it appeared that $Sb(Ph)_4$(ECO) had some form of antifungal activity, but all other compounds were not promising in that field.

MIC antifungal activity assay. MIC assays were conducted to show a comparative study of free cyanoximes with an organoantimony(V) cyanoximate against the same fungi strains as disk assays. Results of initial MIC assay in singlet can be seen in Figure 61. Any MICs at 100 μg/mL signified no inhibitory effects. This was the maximum concentration that the lab could identify with their equipment. Considering the results of each free cyanoxime, it is a clear statement that free cyanoximes have no antifungal activity. On the other hand, when the MCO^- cyanoxime anion was coordinated to organoantimony(V) a clear showing of inhibition was recorded. A second run of tests was performed with essentially the same results as the initial MIC assay, except a lower MIC in the case of *Cryptococcus neoformans* (Figure 62). Regardless, if one thing is evident, further studies must be conducted to solidify the practicality of using organoantimony (V) cyanoximates for antifungal treatment.

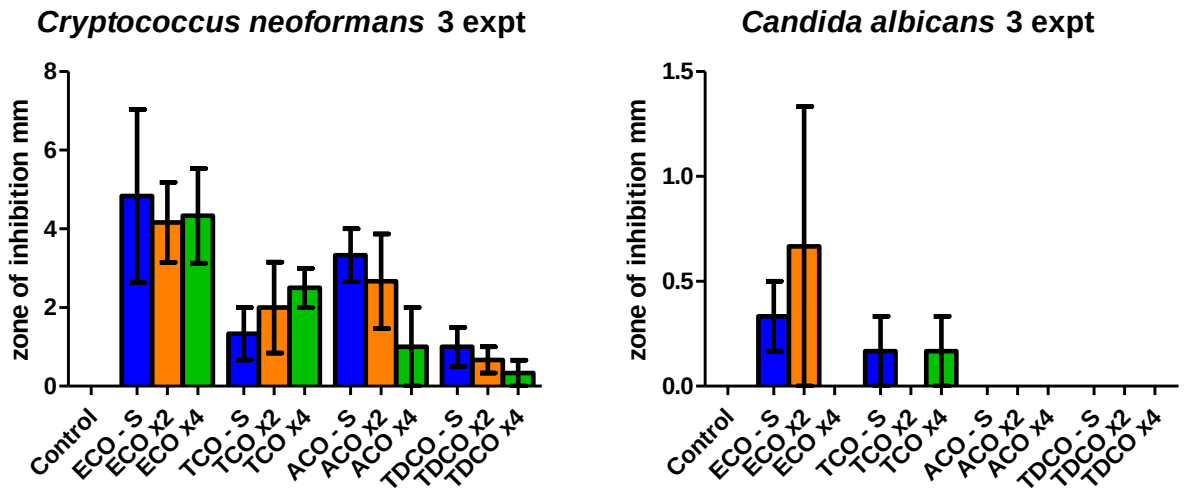

Figure 30. Results of initial disk assays for antifungal activity studies.

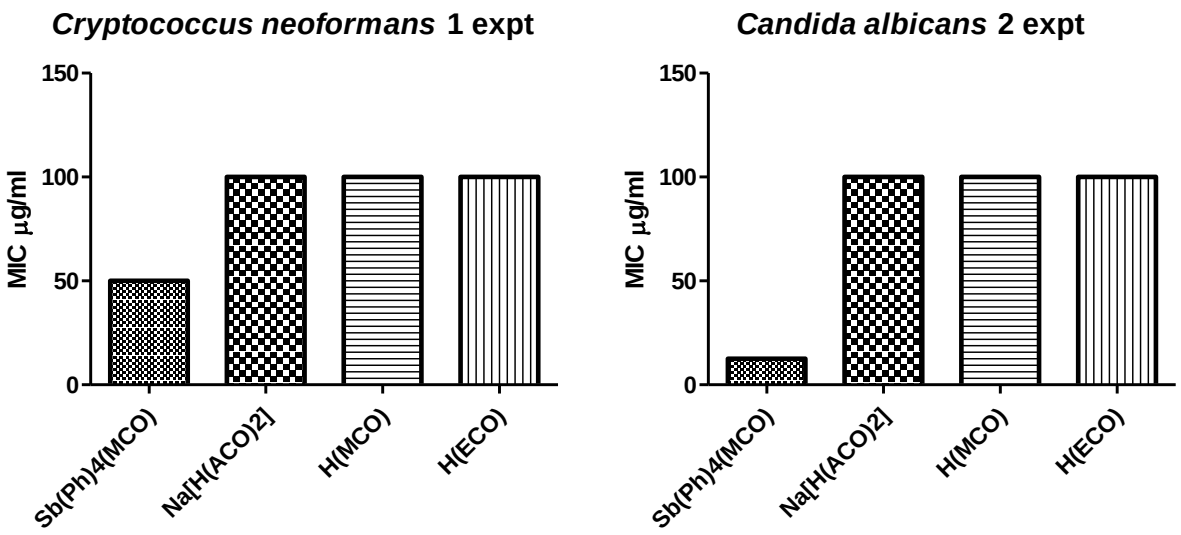

Figure 31. Results of initial MIC assays for antifungal activity studies.

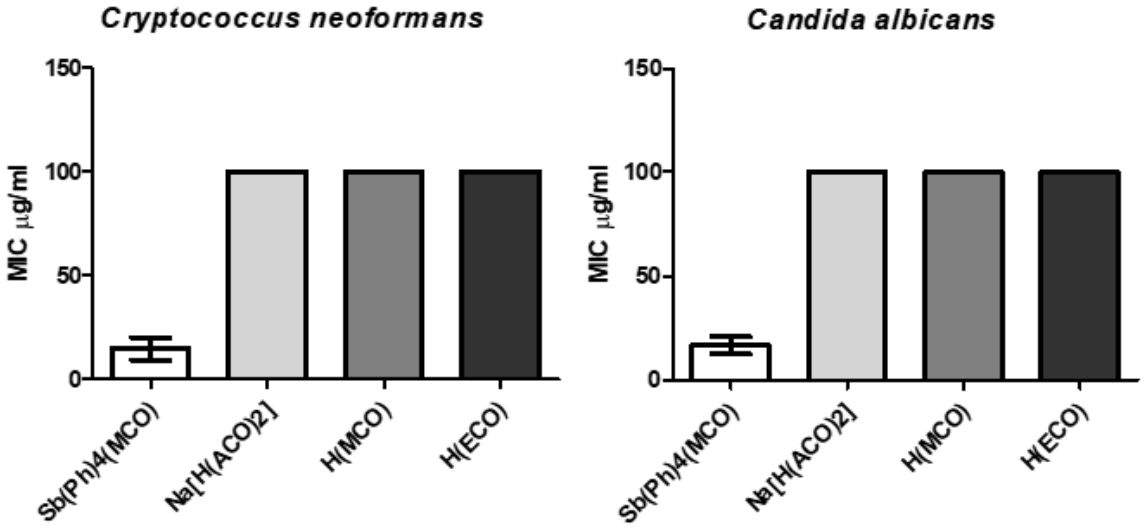

Figure 32. Second round of MIC assays for antifungal activity studies.

CONCLUSIONS AND SUMMARY

Kevin Pink's research project has been carried out within the last three years. As the result of conducted investigation all outlined goals at the beginning of this thesis were accomplished. More specific outcomes are presented as ***chemical*** and ***biological*** results and listed below.

Chemical part:

- Several protonated HL cyanoximes, their Ag(I) (for MCO^-) and Tl(I) (for TCO^-, $TDCO^-$ ligands) derivatives have been synthesized and characterized for the purpose of preparation of new organoantimony(V) cyanoximate-containing compounds.

- Synthesized organoantimony(V) cyanoximates were characterized by elemental analysis, TG/DSC analysis, FT-IR, $^{13}C\{^1H\}$ NMR and, in some cases, variable temperature UV-visible spectroscopy.

- Eight new crystal structures of organoantimony(V) cyanoximates were determined and one previously described in our group compound re-examined second time at low temperature to improve quality of its data. Eight complexes represent mononuclear molecular organometallic compounds and one is a linear μ-oxo dimer with *trans*-positioned cyanoxime moieties (case with ECO^- ligand).

- Two polymorphs were observed in the $Sb(Ph)_4(TCO)$ system and their origin relates to the crystallization method. Three structures out of nine contain multiple crystallographically independent molecules in the asymmetric unit (ASU): two in structures of $Sb(Ph)_4(ECO)$ and $Sb(Ph)_4(MCO)$ and *eight* in the structure of second polymorph of $Sb(Ph)_4(TCO)$.

- In all nine oganoantimony(V) cyanoximates central atom is in pentavalent state and has distorted trigonal bipyramid environment comprising of four carbon atoms of the phenyl groups and one oxygen atom of the cyanoxime anion bound to a Sb(V) center in a monodentate manner.

- All synthesized compounds are well soluble in common organic solvents and poorly soluble in water and aqueous buffers. All solutions in organic solvents are stable over time and demonstrate negligible dissociation due to ionization at elevated temperatures above 60^oC.

Biological part:

- Two kinds of antimicrobial activity tests were carried out for selected new organoantimony(V) cyanoximates: 1) based on paper disks with solid compounds on solid media determination of zone of inhibition, and 2) determination of the minimal inhibitory concentration (MIC) in solutions of compounds.

- Five Sb(V) cyanoximates: $Sb(Ph)_4(ACO)$, monomeric $Sb(Ph)_4(ECO)$, $Sb(Ph)_4(MCO)$, $Sb(Ph)_4(TCO)$, and $Sb(Ph)_4(TDCO)$ were selected at the beginning of antimicrobial and

antifungal studies via paper disk susceptibility and MIC assays. The rational for choices were: a) ACO^-, ECO^- and MCO^- cyanoxime anions possess some water solubility and are rich on oxygen donor atoms; b) TCO^- and $TDCO^-$ are thioamides. Therefore, there is a chance of making structure-activity-relationship (SAR) comparing analogous *oxo*- and *thio*-cyanoximes. The control compound was the initial $Sb(Ph)_4Br$ compound without cyanoximes. Also, pure ligands such as H(MCO), H(ECO) and $Na\{H(ACO)\}_2$ without Sb-atoms were used as a second set of controls.

- Antimicrobial paper disk studies indicated that $Sb(Ph)_4(ACO)$, $Sb(Ph)_4(ECO)$, have ***significant antimicrobial effect*** against all three employed strains: two gram-negative *Escherichia coli* strain S17 and *Pseudomonas aeruginosa* strain PAO1, alongside a single gram-positive Methicillin-resistant *Staphylococcus aureus* strain NRS70.

- $Sb(Ph)_4(TCO)$ and $Sb(Ph)_4(TDCO)$ had ***significant effects*** on the gram- positive Methicillin-resistant *Staphylococcus aureus* strain NRS70, but essentially <u>*no antimicrobial activity*</u> for gram-negative strains used, which we found to be very interesting.

- MIC assay results indicated that free cyanoximes have no antimicrobial effect, but the DMSO solvent used in these assays contributed to the inhibition factor to the MIC assay on cell cultures in solutions.

- Antifungal disk assays were studied with the compounds $Sb(Ph)_4(ACO)$, $Sb(Ph)_4(ECO)$, $Sb(Ph)_4(TCO)$, and $Sb(Ph)_4(TDCO)$ against the fungi of *Cryptococcus neoformans* and *Candida albicans* strains. Disk assays concluded that $Sb(Ph)_4(ECO)$ was effective against *Cryptococcus neoformans* and *Candida albicans* in a positive trend. $Sb(Ph)_4(TCO)$ was the next contributor towards antifungal activity against both strains. $Sb(Ph)_4(ACO)$ and $Sb(Ph)_4(TDCO)$ were only effective at inhibition of *Cryptococcus neoformans*, while those compounds did not contribute to any inhibition towards *Candida albicans*.

- Antifungal MIC assays were conducted on the same strains as the disks assays and used the same Sb(V) cyanoximate $Sb(Ph)_4(MCO)$ along with the free ligands H(MCO), H(ECO), and $Na[H(ACO)_2]$. Results indicated that the free, uncomplexed cyanoximes had zero effect on antifungal activity in both replicas of the experiment. On the other hand, $Sb(Ph)_4(MCO)$ had shown MIC levels ranging from 10 - 50 μg/mL, proving there is ***antifungal activity*** with this organometallic complex.

Travel!

During Kevin's work in my research laboratory we did travel to several locations. One of those was a group tour to Bridal Cave and Ha-Ha-Tonka state park in October of 2019.

Kevin also attended Regional and National Meetings of the ACS.

In January of 2020 together with Seth Adu we traveled to collaborator's research laboratories in Stillwater, OK. We met with all people involved in biological testing of our compounds!

GRADUATION!